



# Synthesis of novel dimeric compounds containing triazole using click method and their selective antiproliferative and proapoptotic potential via mitochondrial apoptosis signaling

H. R. Ferhat Karabulut<sup>1</sup> · Ali Osman Karatavuk<sup>1</sup> · Hasan Ozyildirim<sup>2</sup> · Oğuzhan Doğanlar<sup>3</sup> · Zeynep Banu Doğanlar<sup>3</sup>

Received: 8 November 2019 / Accepted: 15 January 2020  
© Springer Science+Business Media, LLC, part of Springer Nature 2020

## Abstract

In this study, the main aim was synthesis of dimeric compounds, which contain lithocholic acid and a triazole structure to investigate the selective cellular and molecular antiproliferative and proapoptotic potential of these products in healthy embryonic fibroblast (MEF), cervix cancer (HeLa), and breast cancer (MCF-7) cells. Four ester (**5a–d**) and five dimeric (**6a–d**, **7**) out of nine novel compounds were obtained. First of all, lithocholic acid was converted to methyl lithocholate and then it was reacted with certain alkynoic acids (**a–d**) to obtain its alkynoate derivatives (**5a–d**). Finally, these compounds were converted to dimers (**6a–d**) by using 2,6-bis(azidomethyl)pyridine via the click method. Our result indicate that, treatment with dimeric compounds can selectively decrease the cell viability and proliferation in cervix cancer HeLa and breast cancer MCF-7 cells, except **7** which caused a strong cytotoxicity on healthy MEF cells. According to MTT assay, Nucblue cell stain and Annexin V/Propidium iodide molecular probe staining, 100  $\mu\text{M}$  concentrations of the dimeric compounds was sufficient in inducing death and apoptotic cell ratio in HeLa and MCF-7 breast cancer cells selectively. In brief, the present study indicates that most effective dimeric compounds are **6a** and **6b**, which have the highest  $\text{IC}_{50}$  (345.8–342.6  $\mu\text{M}$ ) value on healthy cell and the lowest  $\text{IC}_{50}$  value in both cervix (49.2–36.9  $\mu\text{M}$ ) and breast (23.0–66.1  $\mu\text{M}$ ) cancer cells especially long-term treatment and which triggers apoptosis pathway specifically.

**Keywords** Click chemistry · Lithocholic acid · HeLa · MCF-7 · Gene expression

## Introduction

Heterocyclic compounds are very important in synthetic chemistry. Heterocyclic compounds containing the nitrogen atom especially are widely used. One of the heterocyclic compound classes is triazole derivative compounds. As

click chemistry has developed (Himo et al. 2002, 2005; Kolb and Sharpless 2003; Malkoch et al. 2005; Rostovtsev et al. 2002; Morales-Sanfrutos et al. 2008), the synthesis of 1,2,3-triazole derivative heterocyclic compounds and studies utilizing these compounds have increased. 1,2,3-triazole derivatives attract special interest due to their biological activity and structural properties in medicine and material science. In addition to their anticancer activity (Kádár et al. 2012; Nagesh et al. 2015; Rahman et al. 2017; Reddy et al. 2018), they are also known to show antimicrobial (Vatmurge et al. 2008; Yadav et al., 2018), antifungal (Tan et al. 2017; Lima-Neto et al. 2012), antiviral (Glowacka et al. 2013; Asif 2017), antituberculosis (Menendez et al. 2011), and anti-HIV (Vasilyeva et al. 2017; Chen et al. 2015) activity. In addition, these 1,2,3-triazoles are utilized in the dye industry (Duan et al. 2012) and production of herbicides (Nejma et al. 2018).

Bile acids are important natural compounds with amphiphilic properties due to their skeleton and physiological functions (Anandkumar and Rajakumar 2017).

**Supplementary information** The online version of this article (<https://doi.org/10.1007/s00044-020-02510-x>) contains supplementary material, which is available to authorized users.

✉ H. R. Ferhat Karabulut  
fkarabulut@trakya.edu.tr

<sup>1</sup> Department of Chemistry, Faculty of Science, Trakya University, 22030 Edirne, Turkey

<sup>2</sup> Department of Mathematics and Science Education, Faculty of Education, Trakya University, 22030 Edirne, Turkey

<sup>3</sup> Department of Medical Biology, Faculty of Medicine, Trakya University, 22030 Edirne, Turkey

Among the bile acids, the structure with the highest lipophilic character is lithocholic acid. Lithocholic acid is mainly produced by gut microbiota, and effective in regulating biological events such as activating the vitamin D receptor (Ahmad and Haeusler 2019). In addition, lithocholic acid has an antiproliferative effect by inducing apoptosis in breast cancer cells (Luu et al. 2018), and has selective cytotoxicity to childhood brain tumor and human prostate cancer cells at acceptable concentrations without affect healthy cells (Goldberg et al. 2011, 2013). In LNCaP and PC-3 prostate cancer cells, lithocholic acid triggers both death receptors associated apoptosis signals and caspase-dependent mitochondrial pathways of apoptotic cell death via decrease in the mitochondrial protein Bcl-2 and cleavage of Bax, concomitant with an increase of mitochondrial outer membrane permeability (Gafar et al. 2016). Qiao et al. (2001) found that bile acids enhance caspases-3 and -9 cleavage and triggers mitochondrial apoptosis in two different types of colon carcinoma HT29 and HCT-116 cells. Apoptotic induction with some lithocholic acid derivatives via cleavage of Mcl-1 (Myeloid Cell Leukemia-1) and PARP-1 (Poly(ADP-Ribose)Polymerase-1) as well as the hyperphosphorylation of I $\kappa$ B $\alpha$ , an inhibitor of NF $\kappa$ B (nuclear factor- $\kappa$ B) were reported in KMS-11 human myeloma cell lines (El Kihel et al. 2008). He et al. (2017) reported that lithocholic acid derivatives have stronger antitumor activity than lithocholic acid. There are also various biological applications of lithocholic acid derivatives as antibacterial activity (Nascimento et al. 2015), proteasome regulators (Dang et al. 2012), radiopharmaceutical (Campazzi et al. 1999), and sialyltransferase inhibitors (Abdu-Allah et al. 2016). Also, the synthesis of dimeric bile acids and dimeric steroids has been of interest to researchers due to their different application areas. Jurášek et al. (2013), reacted cholic acid with propargyl bromide from the carboxylic acid group to obtain triazole-derived dimers and examined their hormone receptor activities. Triazole containing dimeric estrones were synthesized for the synthesis of tetrameric estrone based macrocyclic compounds (Ramírez-López et al. 2008).

Nowadays, cancer is one of the most challenging diseases, which may result in death. According to the literature, breast cancer was the most widespread type of cancer in women in 2018, followed by colorectal, lung, and cervix uteri cancer (WCRF 2018). Therefore, studies on the development of new cancer drugs have always attracted the attention of scientists. As mention above, lithocholic acid and triazole derivative compounds are exhibit biological activities. For this reason, the novel dimers, containing lithocholic acid and triazole moieties (**6a–d**) were synthesized using click method. First of all, lithocholic acid was converted to methyl lithocholate for the synthesis of dimeric compounds. Then it was reacted from its 3-OH position

with different alkynoic acids (**a–d**) to obtain its terminal alkynoate derivatives (**5a–d**). These compounds were converted to dimers (**6a–d**) by using 2,6-bis(azidomethyl)pyridine via the click method. Then the antiproliferative and proapoptotic effect of the obtained dimeric compounds at molecular and cellular levels in the HeLa and MCF-7 cancer cell lines (**6a–d**, **7**) was examined, and the results were compared with normal cell MEF. The reason for the use of bile acid in this study is its biological activity and its ability to penetrate the cell membrane due to its amphiphilic properties. The aim was to synthesize the novel dimers and to investigate the effect of dimers with different carbon numbers on antiproliferative and proapoptotic activity. Compound **7** was also synthesized to study the effect of lithocholic acid on cytotoxic activity.

## Materials and methods

### Chemistry

All chemical reagents and solvents were purchased from Merck, Acros, and Sigma-Aldrich and used without any purification. Solvents were dried with a 3 Å molecular sieve, activated, and used at analytical grade. Varian Mercury Plus 300 MHz was used for  $^1\text{H}$  and  $^{13}\text{C}$  NMR spectra. Chemical shift values ( $\delta$ ) are given in parts per million (ppm). Perkin Elmer Frontier was used for FT-IR spectra. Waters SYNAPT G1 MS was used for the HR-MS results. Thin-layer chromatography (TLC) was performed on silica gel GF254. Silica gel 60 purchased from Merck was used for the column chromatography.

### Synthesis of 2,6-Bis(azidomethyl)pyridine (**2**)

2,6-Bis(bromomethyl)pyridine (1.0 g, 3.77 mmol) was dissolved in 20 mL of DMSO. Sodium azide (0.61 g, 9.43 mmol) was added to the mixture and stirred at room temperature for 24 h. The reaction was quenched with 30 mL of ice water. The reaction mixture was extracted with ethyl acetate. In the organic phase it was washed three times with 40 mL of water and then dried with  $\text{Na}_2\text{SO}_4$ . The organic solvent was evaporated in a vacuum. Yield: 91%. IR ( $\text{cm}^{-1}$ ): 2059.  $^1\text{H}$  NMR (300 MHz,  $\text{CDCl}_3$ ):  $\delta$  ppm 7.75 (t,  $J = 7.8$  Hz, 1H), 7.30 (d,  $J = 7.6$  Hz, 2H), 4.48 (s, 4H).

### Synthesis of Methyl 3 $\alpha$ -hydroxy-5 $\beta$ -cholane-24-oate (**4**)

Into the flask placed in an ice bath was added lithocholic acid (1.17 g, 3.0 mmol) and 20 mL methanol. Acetyl chloride (1.07 mL, 15 mmol) was added to the solution. The reaction was stirred for 24 h in an ice bath. Water was added to the reaction mixture. The resulting precipitate of methyl

lithocholate was filtered off and dried without further purification. Yield: 98%. White crystal. mp: 128.9–129.2 °C (lit. mp :129 °C). IR (cm<sup>-1</sup>): 3475, 1728. <sup>1</sup>H NMR (300 MHz, CDCl<sub>3</sub>): δ ppm 3.47–3.77 (m, 4H), 2.13–2.45 (m, 2H), 1.00–2.02 (m, 27H), 0.87–0.97 (m, 6H), 0.62–0.70 (m, 3H). <sup>13</sup>C NMR (75 MHz, CDCl<sub>3</sub>): δ ppm 174.7, 71.6, 56.3, 55.8, 51.4, 42.6, 42.0, 40.3, 40.0, 35.7, 35.2, 35.3, 34.4, 30.9, 30.8, 30.4, 28.0, 27.1, 26.3, 24.1, 23.3, 20.7, 18.1, 11.9.

### General procedure for esterification of methyl lithocholate by alkynoic acids (5a–d)

Alkynoic acid (2.56 mmol) (a–d) was dissolved in CH<sub>2</sub>Cl<sub>2</sub> (20 mL). DCC/DMAP solution was prepared by dissolving DCC (2.56 mmol) and DMAP (2.56 mmol) in CH<sub>2</sub>Cl<sub>2</sub> (20 mL). To a solution of methyl lithocholate (1.28 mmol) in 20 mL of CH<sub>2</sub>Cl<sub>2</sub> that was cooled to 0 °C was added half of an alkynoic acid solution and this was followed by the dropwise addition of half a DCC/DMAP solution. The mixture was stirred at 0 °C for 5 min, then the rest of the acid solution was quickly added, followed by the dropwise addition of the rest of the DCC/DMAP solution. The reaction mixture was stirred 10 min for **5a** and 1 h for **5a–d** at 0 °C, after which the reaction was quenched with water. The organic phase was separated. The water phase was extracted twice with 20 mL of CH<sub>2</sub>Cl<sub>2</sub>. The organic phases were collected and dried over MgSO<sub>4</sub>. The organic phase was evaporated in a vacuum. Residue was purified using column chromatography in Ethyl acetate/n-Hexane (1/20).

#### Methyl 3α-propynoyloxy-5β-cholane-24-oate (5a)

Yield: 19%. White crystal. Rf: 0.17. mp: 176–178 °C. IR (cm<sup>-1</sup>): 3241.2, 2114.6, 1730.0, 1709.2. <sup>1</sup>H NMR (300 MHz, CDCl<sub>3</sub>): δ ppm 4.71–5.00 (m, 1H), 3.68 (s, 3H), 2.87 (s, 1H), 2.15–2.46 (m, 2H), 1.69–2.03 (m, 7H), 1.00–1.68 (m, 19H), 0.87–0.99 (m, 6H), 0.65 (s, 3H). <sup>13</sup>C NMR (75 MHz, CDCl<sub>3</sub>): δ ppm 175.0, 152.5, 75.4, 74.3, 56.7, 56.2, 51.7, 43.0, 42.1, 40.6, 40.4, 36.0, 35.6, 35.2, 34.8, 32.2, 31.3, 31.2, 28.4, 27.2, 26.6, 26.5, 24.4, 23.5, 21.1, 18.5, 12.3. HR-MS (ESI): m/z 465.2983 [M+Na]<sup>+</sup> (calcd for C<sub>28</sub>H<sub>42</sub>O<sub>4</sub>Na; 465.2981).

#### Methyl 3α-(4-pentynoyloxy)-5β-cholane-24-oate (5b)

Yield: 79%. White crystal. Rf: 0.18. mp: 120–122 °C. IR (cm<sup>-1</sup>): 3308.1, 2121, 1732.5. <sup>1</sup>H NMR (300 MHz, CDCl<sub>3</sub>): δ ppm 4.68–4.85 (m, 1H), 3.68 (s, 3H), 2.47–2.58 (m, 4H), 2.14–2.45 (m, 2H), 0.99–2.03 (m, 27H), 0.87–0.97 (m, 6H), 0.65 (s, 3H). <sup>13</sup>C NMR (75 MHz, CDCl<sub>3</sub>): δ ppm 175.0, 171.5, 82.8, 75.0, 69.2, 56.7, 56.2, 51.7, 43.0, 42.1, 40.7, 40.4, 36.0, 35.6, 35.2, 34.8, 33.9, 32.5, 31.3, 31.2,

28.4, 27.2, 26.9, 26.6, 24.4, 23.6, 21.1, 18.5, 14.7, 12.3. HR-MS (ESI): m/z 493.3298 [M+Na]<sup>+</sup> (calcd for C<sub>30</sub>H<sub>46</sub>O<sub>4</sub>Na; 493.3294).

#### Methyl 3α-(5-hexynoyloxy)-5β-cholane-24-oate (5c)

Yield: 76%. White crystal. Rf: 0.18. mp: 66–67 °C. IR (cm<sup>-1</sup>): 3289.5, 2120, 1733.6. <sup>1</sup>H NMR (300 MHz, CDCl<sub>3</sub>): δ ppm 4.49–4.94 (m, 1H), 3.67 (br. s, 3H), 2.42 (t, J = 7.32 Hz, 2H), 2.16–2.39 (m, 4H) 1.01–2.05 (m, 29H) 0.86–0.98 (m, 6H) 0.65 (s, 3H). <sup>13</sup>C NMR (75 MHz, CDCl<sub>3</sub>): δ ppm 175.0, 172.8, 83.6, 74.6, 69.3, 56.7, 56.2, 51.7, 43.0, 42.1, 40.6, 40.3, 36.0, 35.6, 35.3, 34.8, 33.6, 32.5, 31.2, 28.4, 27.2, 26.9, 26.5, 24.4, 24.0, 23.6, 21.1, 18.5, 18.1, 12.3. HR-MS (ESI): m/z 507.3471 [M+Na]<sup>+</sup> (calcd for C<sub>31</sub>H<sub>48</sub>O<sub>4</sub>Na; 507.3450).

#### Methyl 3α-(6-heptynoyloxy)-5β-cholane-24-oate (5d)

Yield: 77%. White crystal. Rf: 0.18. mp: 96–98 °C. IR (cm<sup>-1</sup>): 3265.8, 1737.3, 1723.9. <sup>1</sup>H NMR (300 MHz, CDCl<sub>3</sub>): δ ppm 4.66–4.89 (m, 1H), 3.68 (s, 3H), 2.16–2.48 (m, 6H), 0.85–2.11 (m, 37H), 0.66 (br. s., 3H). <sup>13</sup>C NMR (75 MHz, CDCl<sub>3</sub>): δ ppm 175.1, 173.2, 84.3, 74.5, 68.8, 56.7, 56.2, 51.8, 43.0, 42.1, 40.6, 40.4, 36.0, 35.6, 35.3, 34.8, 34.4, 32.5, 31.3, 31.2, 28.4, 28.1, 27.3, 26.9, 26.6, 24.4, 24.4, 23.6, 21.1, 18.5, 18.4, 12.3. HR-MS (ESI): m/z 499.3793 [M+H]<sup>+</sup> (calcd for C<sub>32</sub>H<sub>51</sub>O<sub>4</sub>; 499.3787).

### General procedure for synthesis of dimer (6a–d)

2,6-Bis(azidomethyl)pyridine (0.38 mmol) was dissolved in 20 mL of DMF, followed by the addition of CuSO<sub>4</sub>·5H<sub>2</sub>O (0.08 mmol), sodium ascorbate (0.15 mmol) and the ester derivative compound (**5a–d**) (0.78 mmol). The solution was stirred at 40 °C for 24 h. The reaction was quenched by adding water. The precipitated solids were filtered off and purified by column chromatography in CH<sub>3</sub>OH/CH<sub>2</sub>Cl<sub>2</sub> (1/20).

#### 2,6-Bis[methyl 5β-cholane-24-oate-3α-yl-formate-1-yl]-1H-1,2,3-triazole-1-yl- methyl] pyridine (6a)

Yield: 86%. White crystal. Rf: 0.74. mp: 130–132 °C. IR (cm<sup>-1</sup>): 1718.6, 1542.0, 1335.9. <sup>1</sup>H NMR (300 MHz, CDCl<sub>3</sub>): δ ppm 8.22 (br. s., 2H), 7.73 (t, J = 7.5 Hz, 1H), 7.19 (d, J = 7.6 Hz, 2H), 5.69 (br. s., 4H), 4.88–5.21 (m, 2H), 3.67 (br. s., 6H), 2.15–2.50 (m, 4H), 0.76–2.15 (m, 64H), 0.65 (br. s., 6H). <sup>13</sup>C NMR (75 MHz, CDCl<sub>3</sub>): δ ppm 175.0, 160.4, 154.3, 141.4, 139.2, 128.3, 122.4, 75.9, 56.7, 56.2, 55.6, 51.7, 43.0, 42.2, 40.5, 40.4, 36.0, 35.6, 35.3, 34.9, 32.4, 31.3, 31.2, 28.4, 27.3, 26.8, 26.5, 24.4, 23.5, 21.0, 18.5, 12.3. HR-MS (ESI): m/z 1074.7012 [M+H]<sup>+</sup> (calcd for C<sub>63</sub>H<sub>92</sub>N<sub>7</sub>O<sub>8</sub> 1074.7007).

**2,6-Bis[methyl 5 $\beta$ -cholane-24-oate-3 $\alpha$ -yl-propanoate-3-yl]-1H-1,2,3-triazole-1-yl-methyl] pyridine (6b)**

Yield 89%. White crystal. Rf: 0.41. mp: 75–77 °C. IR (cm<sup>-1</sup>): 1731.0, 1720.4, 1542.0; 1356.9. <sup>1</sup>H NMR (300 MHz, CDCl<sub>3</sub>):  $\delta$  ppm 7.65 (t, J = 7.6 Hz, 1H), 7.49 (s, 2H), 7.06 (d, J = 7.6 Hz, 2H), 5.61 (s, 4H), 4.60–4.81 (m, 2H), 3.67 (s, 6H), 3.06 (t, J = 7.0 Hz, 4H), 2.72 (t, J = 6.9 Hz, 4H), 2.08–2.45 (m, 4H), 0.75–2.03 (m, 64H), 0.64 (s, 6H). <sup>13</sup>C NMR (75 MHz, CDCl<sub>3</sub>):  $\delta$  ppm 175.0, 172.5, 155.1, 147.3, 138.8, 122.2, 121.8, 74.8, 56.7, 56.2, 55.4, 51.7, 43.0, 42.1, 40.6, 40.3, 36.0, 35.6, 35.2, 34.8, 34.2, 32.5, 31.3, 31.2, 28.4, 27.3, 26.9, 26.5, 24.4, 23.6, 21.3, 21.1, 18.5, 12.3. HR-MS (ESI): m/z 1130.7664 [M+H]<sup>+</sup> (calcd for C<sub>67</sub>H<sub>100</sub>N<sub>7</sub>O<sub>8</sub> 1130.7633).

**2,6-Bis[methyl 5 $\beta$ -cholane-24-oate-3 $\alpha$ -yl-butanoate-4-yl]-1H-1,2,3-triazole-1-yl-methyl] pyridine (6c)**

Yield 84%. White crystal. Rf: 0.44. mp: 76–78 °C. IR (cm<sup>-1</sup>): 1730.5, 1553, 1379. <sup>1</sup>H NMR (300 MHz, CDCl<sub>3</sub>):  $\delta$  ppm 7.68 (t, J = 7.8 Hz, 1H), 7.45 (s, 2H), 7.09 (d, J = 7.6 Hz, 2H), 5.62 (s, 4H), 4.63–4.81 (m, 2H), 3.67 (s, 6H), 2.79 (t, J = 7.3 Hz, 4H), 2.12–2.45 (m, 9H), 0.73–2.10 (m, 67H), 0.65 (s, 6H). <sup>13</sup>C NMR (75 MHz, CDCl<sub>3</sub>):  $\delta$  ppm 175.0, 173.0, 155.1, 148.1, 138.8, 121.8, 74.6, 56.7, 56.2, 55.4, 51.7, 43.0, 42.1, 40.6, 40.3, 36.0, 35.6, 35.3, 34.8, 34.3, 32.5, 31.3, 31.2, 28.4, 27.3, 26.9, 26.5, 25.2, 25.0, 24.4, 23.6, 21.1, 18.5, 12.3. HR-MS (ESI): m/z 1158.7972 [M+H]<sup>+</sup> (calcd for C<sub>69</sub>H<sub>104</sub>N<sub>7</sub>O<sub>8</sub> 1158.7946).

**2,6-Bis[methyl 5 $\beta$ -cholane-24-oate-3 $\alpha$ -yl-petanoate-5-yl]-1H-1,2,3-triazole-1-yl-methyl] pyridine (6d)**

Yield 87%. White crystal. Rf: 0.38. mp: 70–72 °C. IR (cm<sup>-1</sup>): 1729.9, 1554, 1378. <sup>1</sup>H NMR (300 MHz, CDCl<sub>3</sub>):  $\delta$  ppm 7.67 (t, J = 7.6 Hz, 1H), 7.43 (s, 2H), 7.06 (d, J = 7.6 Hz, 2H), 5.62 (s, 4H), 4.59–4.84 (m, 2H), 3.67 (s, 6H), 2.76 (br. s., 4H), 2.12–2.46 (m, 8H), 0.77–2.04 (m, 72H), 0.64 (s, 6H). <sup>13</sup>C NMR (75 MHz, CDCl<sub>3</sub>):  $\delta$  ppm 175.0, 173.3, 155.2, 148.6, 138.8, 121.8, 121.7, 74.5, 56.7, 56.2, 55.4, 51.7, 43.0, 42.1, 40.6, 40.3, 36.0, 35.6, 35.3, 34.8, 34.6, 32.5, 31.3, 31.2, 29.0, 28.4, 27.3, 26.9, 26.5, 25.6, 24.7, 24.4, 23.6, 21.1, 18.5, 12.3. HR-MS (ESI): m/z 1186.8267 [M+H]<sup>+</sup> (calcd for C<sub>71</sub>H<sub>108</sub>N<sub>7</sub>O<sub>8</sub> 1186.8259).

**Synthesis of Pyridine-2,6-diylbis(methylene)bis(1H-1,2,3-triazole-1,4-diy)diacetic acid (7)**

2,6-bis(azidomethyl)pyridine (0.38 mmol), CuSO<sub>4</sub>·5H<sub>2</sub>O (0.08 mmol), sodium ascorbate (0.15 mmol), and 3-butynoic acid (0.95 mmol) were dissolved in 20 mL of DMF and stirred at 40 °C for 24 h. After 24 h, the reaction

was allowed to warm to room temperature and the solvent removed under vacuum. The residue was purified using column chromatography with methanol. Yield 64%. Creamy crystal. Rf: 0.71. mp: 162–164 °C. IR (cm<sup>-1</sup>): 3401.0, 1703.0, 1566.9, 1353.1. <sup>1</sup>H NMR (300 MHz, D<sub>2</sub>O):  $\delta$  ppm 7.65–8.06 (m, 3H), 7.20 (d, J = 7.6 Hz, 2H), 5.66 (br. s., 4H), 3.54 (br. s., 4H). <sup>13</sup>C NMR (75 MHz, D<sub>2</sub>O):  $\delta$  ppm 178.4, 154.4, 143.9, 139.9, 125.1, 122.6, 54.7, 34.2. HR-MS (ESI): m/z 380.1086 [M+Na]<sup>+</sup> (calcd for C<sub>15</sub>H<sub>15</sub>N<sub>7</sub>O<sub>4</sub>Na 380.1083).

**Cells and chemicals**

Two cancer cell lines, human cervix adenocarcinoma HeLa (ATCC® CCL-2™) and human breast adenocarcinoma MCF7 (ATCC® HTB-22™), and one healthy cell mouse embryonic fibroblast MEF (CF-1) (ATCC® SCRC-1040™) were obtained from ATCC (USA). The whole experiment was carried out in DMEM: F-12 Medium (ATCC® 30-2006™), including heat-inactivated 10% FBS (Multicell), 2 mM glutamine (Gibco-Life Technologies), and 1% Pen-Strep (Multicell). The cancerous and healthy cells were cultured at 37 °C and 5% CO<sub>2</sub>. Cell culture experiments were started for all cells in the 5th passage and finished in the 20th. The MTT reagent [3-(4,5-Dimethylthiazol-2-yl)-2,5-Diphenyltetrazolium Bromide], cell grade ultrapure water, NucBlue™ Live ReadyProbes™ Reagent, a Tali® Apoptosis Kit—Annexin V Alexa Fluor® 488 and Propidium Iodide cell apoptosis kit, the PureLink® RNA Mini Kit, a High Capacity cDNA Reverse Transcription Kit and Power SYBR® Green Master Mix were purchased from Thermo Fisher Scientific.

**Cell proliferation assay (MTT)**

The effect on cell viability of dimeric compounds (6a–d, 7) was assayed by a MTT test. Homo sapience adenocarcinoma-type cell lines, HeLa and MCF7, and normal cells MEF were used in the experiment. The cervix cancer HeLa (3000 cells/well), breast cancer MCF7 (5000 cells/well) and embryonic fibroblast MEF (2000 cells/well) were seeded into 96-well cell culture-type plates and were incubated at 37 °C for 12 h in a humidified incubator containing 5% CO<sub>2</sub>. After an incubation period in cell culture media to permit cell attachment, the control group treated vehicle (1% DMSO + ultrapure water) and experimental groups were treated with serial sixfold dilutions (15.62–500  $\mu$ M) of dimeric compounds (6a–d, 7) diluted in cell culture grade ultrapure water. Both the vehicle control and experimental groups were incubated for up to 48 h, and six replicates were conducted for each 24 and 48 h time-point. When the time was completed, a 20  $\mu$ l MTT solution was pipetted using a micropipette in each

well (5 mg/ml concentration) and the plates were incubated for 4 h at 37 °C. The blue formazan crystals were liquefied in ultrapure DMSO (200  $\mu$ l/well) and were used for dissolving the blue formazan, which was then evaluated at 490 nm with a spectrophotometer (Multiscan Go Microplate Reader, Thermo Scientific, USA). IC<sub>50</sub> values were calculated by the Probit analysis options of SPSS 20 software.

### Molecular fluorescent apoptosis detection assay

We used NucBlue® Live ReadyProbes® Reagent to observe cell nucleus morphology for apoptosis stimulation. For this purpose, 24-well plates were divided into six groups for each cell, and cells were seeded on the well surface at 2–6  $\times$  10<sup>4</sup> cells/well. After 24 h, the control and experiment cells were treated with vehicle and 100  $\mu$ M of dimeric compounds (**6a–d**, **7**), respectively. After 48 h of incubation, live cells in DMEM:F12 medium were labeled with four drops of NucBlue® Live ReadyProbes® Reagent (Thermo Scientific ready). After 30 min, all cells were washed in duplicate with PBS and were observed and imaged at 40 $\times$  magnification on a Zeiss Axio Vert.A1 fluorescent microscope with a DAPI filter.

The rate of apoptotic and necrotic cells treated with derivatives was evaluated by a Tali™ Image-Based Cytometer assay using Annexin V and PI (Tali® Apoptosis Kit; Life Technologies) according to the manufacturer's instructions with minor modification (Guclu et al. 2018). Live, dead (PI+) and apoptotic cells (Annexin V+, and Annexin V+: PI+) were counted and calculated by Tali® Image-Based Cytometer software with apoptosis options.

### Gene expression assay

The gene expression assay was isolated from three cell lines cultured in a 25 cm<sup>2</sup> flask using the PureLink® RNA Mini Kit (Life Technologies, USA), according to the manufacturer's instructions. The RNA concentrations were measured using Optizen NanoQ (Korea). For synthesis of the first strand of cDNA using a High Capacity cDNA Reverse Transcription Kit (Life Technologies, USA), cDNA synthesis was performed using the thermal cycler Applied Biosystems® Veriti® (Step 1: 25 °C, 10 min; Step 2: 37 °C, 120 min; Step 3: 85 °C, 5 min). The cDNA was stored at –20 °C for the qRT-PCR analysis. Gene expression levels of tumor suppressor (P53; F: 5'-CAC GAGCGCTGCTCAGATAGC-3', R: 5'-ACAGGCACAA ACACGCACAAA-3'), B-cell lymphoma 2 (BCL2; F: 5'-ATGTGTGTGGAGAGCGTCAA-3', R: 5'-ACAGTTCCAC AAAGGCATCC-3'), BCL2 associated X (BAX; F: 5'-TTCATCCAGGATCGAGCAGA-3', R: 5'-GCAAAGTAGA AGGCAACG-3'), cytochrome complex (Cyt-C; F: 5'-AGT GGCT AGAGTGGTCATTCATTACA-3', R: 5'-TCAT

GATCTGAATTCTGGTGTATGAGA-3'), apoptotic protease activating factor1 (APAF 1; F: 5'-GATATGGAATG TCTCAGATGGCC-3', R: 5'-GGTCTGTGAGGACTCCC CA-3') and caspase 3 (Casp 3; F: 5'-GGTATTGAGAC AGACAGTGG-3', R: 5'-CATGGGATCTGTTTCTTTGC-3') genes in plated MEF, HeLa, and MCF7 cells treated with EDS were analyzed by qRT-PCR using the Power SYBR® Green Master Mix (Life Technologies, USA) on an ABI Quant Studio 5 Real-Time PCR system using the following PCR condition: 1 cycle of 2 min at 50 °C and 10 min at 95 °C followed by 40 cycles of denaturation at 95 °C for 15 s, annealing and extension at 60 °C for 1 min.

### Statistical analysis

The IC<sub>50</sub> values were calculated with Probit analyses using SPSS 20 software. The mRNA expressions were calculated using the comparative cycle threshold (2<sup>- $\Delta\Delta$ Ct</sup>) method and given as the relative fold change compared with the control and normalized with GAPDH mRNA expression. In addition, differences in the leave, death and apoptotic cell count derive from the Tali assay and the relative fold change levels of gene expressions were compared using one-way analysis of variance (oneway-ANOVA) with Duncan's separation of means test using SPSS 20 software ( $p \leq 0.05$ ).

## Results and discussion

### Chemistry

In our study, 2,6-bis(azidomethyl)pyridine (**2**) used as a linker was synthesized with a yield of 91% in according to the procedure (Narayanaswamy et al. 2011) in the literature (Fig. 1). The peak of azide at 2059 cm<sup>-1</sup> in the IR spectrum confirmed the accuracy of the structure.

Methyl lithocholate was obtained for the synthesis of terminal alkyne derivative esters to be used in the click reaction. For this purpose, lithocholic acid (**3**) was reacted with acetyl chloride in methanol and converted to methyl lithocholate (**4**) at 98% yield.

For obtaining their terminal alkyne derivatives, this compound (**4**) was reacted with propynoic acid (**a**), 4-pentynoic acid (**b**), 5-hexynoic acid (**c**), and 6-heptynoic acid (**d**) by using DCC/DMAP methods (Fig. 2). Ester derivatives (**5a–d**) afforded 19, 79, 76, and 77% yield,

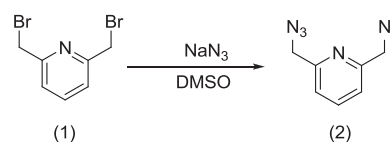


Fig. 1 Synthesis of 2,6-Bis(azidomethyl)pyridine (**2**)

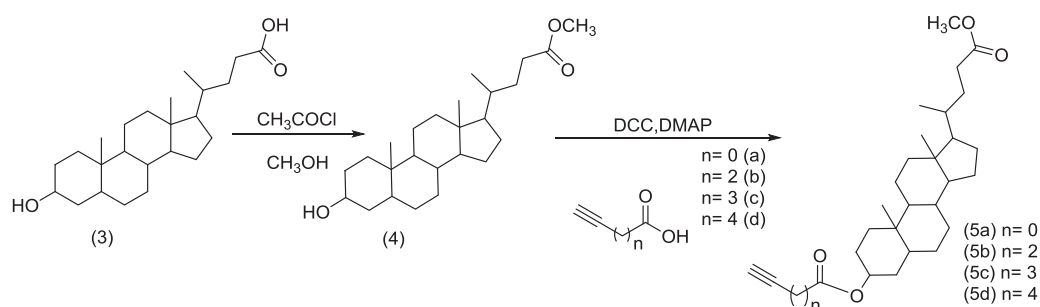


Fig. 2 Esterification of lithocholic acid

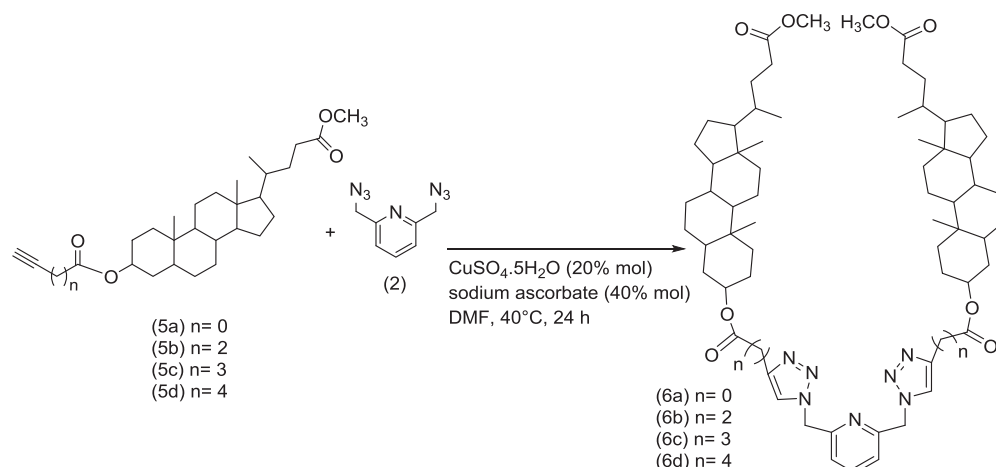


Fig. 3 Dimerization of lithocholic acid derivatives via click reaction

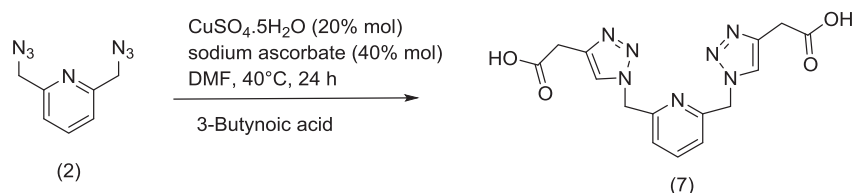
respectively. In the esterification reaction with propionic acid, it was found that the yield was lower than the other compounds (**5b–d**) because of Michael-type additions. The structure of the compounds was confirmed by NMR, IR and mass spectroscopy. In the  $^1\text{H}$  NMR spectrum, the shift of C3 hydrogen from 3.47–3.77 ppm to 4.5–5.0 ppm indicates that alkyne esters (**5a–d**) had occurred. Unlike the others, the alkyne proton of compound **5a** was observed at 2.86 ppm. In the  $^{13}\text{C}$ -NMR spectra of the obtained compounds, different from the starting material, the formation of new carbonyl peaks of 152 and 172 ppm for **5a** and **5b–d**, respectively, confirms the structure. In addition, peaks at 75 and 83 ppm, which belong to alkyne carbons, were observed for **5b–d** in the  $^{13}\text{C}$ -NMR spectrum. In the IR spectrum, an ester carbonyl peak at  $1730\text{ cm}^{-1}$  and alkyne peak at  $3240\text{--}3300\text{ cm}^{-1}$  confirmed the structure. Apart from this spectral analysis, HR-MS analyses were carried out for the **5a–d** compounds and their structures were confirmed with a difference of 0.2: 0.4: 2.1 and 0.6 mDa when their molecular weight is compared. The esterification reaction of methyl lithocholate with 3-butynoic acid resulted in allene derivative ester, instead of its butynoate esters.

Finally, the dimers (**6a–d**) were obtained using the click method. For this purpose, the alkyne-derived compounds

(**5a–d**) were reacted with compound **2** in the presence of copper sulfate and sodium ascorbate to form dimers (**6a–d**) containing a 1,2,3-triazole skeleton (Fig. 3). Final products (**6a–d**) were afforded at 86, 89, 84, and 87% yield, respectively. In the  $^1\text{H}$ -NMR spectrum, the presence of CH protons of the triazole ring at 8.2 ppm for **6a** and 7.4 ppm for **6b–d**, also the shifting of the pyridine-bounded methylenes from 4.48 to 5.6 ppm indicates the formation of the triazole structure. In the  $^{13}\text{C}$ -NMR spectrum, the carbons of the triazole (**6a–d**) in addition to the pyridine and carbonyl peaks in the starting materials were observed at about 122 and 138 ppm. In the infrared spectrum of **6a–d**, the disappearance of the peaks of  $\text{N}_3$  at  $2059\text{ cm}^{-1}$  in the azide compound and peak of  $3240\text{--}3300\text{ cm}^{-1}$  in the alkyne ester confirmed the structure. The mass differences between theoretically-calculated and experimental data were 0.5; 3.1; 2.6 and 0.8 mDa, respectively for the compounds (**6a–d**). Spectral data confirmed that the targeted compounds were successfully synthesized.

Furthermore, in order to find out the effect of the presence of lithocholic acid moiety on anticancer activity compound **7**, which does not contain lithocholic acid, it was synthesized and evaluated (Fig. 4). For this purpose, 2,6-Bis (azidomethyl)pyridine was converted to dimer (**7**) via click

**Fig. 4** Synthesis of pyridine-2,6-diylbis(methylene)bis(1H-1,2,3-triazole-1,4-diyl) diacetic acid (**7**) via click reaction



reaction. From the  $^1\text{H-NMR}$  spectrum of the obtained compound, the shift of the pyridine-bound methylenes from 4.48 to 5.66 ppm and the presence of methylene protons adjacent to the carbonyl carbon at 3.54 ppm indicates that the triazole structure has been formed. In the  $^{13}\text{C-NMR}$  spectra of Compound **7**, pyridine and carbonyl peaks were observed at 178.4, 154.4, 143.9, 139.9, 125.1, and 122.6 ppm in addition to the two carbon peaks of the triazole ring. In the IR spectrum, disappearance of the azide peak at  $2089 \text{ cm}^{-1}$  in compound **2** and the difference of 0.3 mDa in the mass analysis confirm that the structure was obtained.

The purities of steran ring-containing dimeric compounds were verified by qNMR analysis and found to be in the range of 96.14 to 99.93%. Purity analysis for compound **7** was carried out by using HPLC and found to be 100%.

## Biological evaluations

The first step in comprehending the effect of dimeric compounds (**6a–d**, **7**) in this study was to assess the effect of dimeric compounds on healthy and cancer cell viability. Following the application with increasing concentration of dimeric compounds at 24 and 48 h timings, cells were incubated with MTT test solution, which is processed into a violet crystal product by live cells by dynamic metabolism. We determined the effectiveness of the dimeric compounds in decreasing the viability of both cervix and breast adenocarcinoma cells (HeLa and MCF-7) without affecting healthy cells, except at high doses. This effect was dose dependent. A noticeable effect of lithocholic acid and its derivatives is cytotoxic, anticancer characteristics on the cancer cell line (He et al. 2017; Hryniewicka et al. 2018). Indeed, dimeric compounds had a significant effect on the viability and proliferation of both cancerous lines in our panel. In HeLa cells, treatment with 26.07–62.69  $\mu\text{M}$  dimeric compounds for 24 h was sufficient to cause most cells to kill (Fig. 5); whereas in other cancer cell lines, significant effects required higher doses of dimeric compounds (32.75–208.87  $\mu\text{M}$ ) (Fig. 5) or longer exposure (Fig. 6). The MEF cell line was affected significantly less than the HeLa and MCF-7 cells by the same treatment dose and time. Results of the MTT test and  $\text{IC}_{50}$  values of the dimeric compounds on our panel are shown in Figs 5 and 6.

To further evaluate the anticancer properties of the dimeric compounds, we investigated their role in cellular

death mechanisms and their selective capability against cancer cells, using a molecular probe staining method detected by image-based cytometry. In this assay, phosphatidylserine, located at the cytoplasmic side of the cell membrane in living cells, is migrated to the outer membrane during apoptosis. Phosphatidylserine on the outer membrane was stained with Annexin V and this apoptotic cell was green irradiated. The propidium iodide (PI) irradiated red signals and stained only death cells (Luchetti et al. 2006; Salucci et al. 2014). Although cell cultures provide important data for drug development studies, it is often necessary to use a higher dose in human tissue to fight cancer, in order to overcome the defense mechanisms of the organism. In cancer treatments, the most important condition for determining the drug dose is for the drug to have the ability to destroy cancerous tissue, without damaging healthy cells. Therefore, we used a 100  $\mu\text{M}$  dose, which is higher than that of the determined  $\text{IC}_{50}$  doses induce a significant death in cancer cells without damaging healthy cells. Our results demonstrate that dimeric compounds selectively trigger both apoptotic and necrotic cell death in both cervix and breast cancer cells in a dose-dependent manner, as indicated by the increase in Annexin V and propidium iodide positive cells incubated with dimeric compounds (Fig. 7). Our analysis showed a 10.8–44.5% (in HeLa) and 13.5–41.8% (in MCF-7) increase in Annexin V+ cells (apoptotic cells) and a maximum increase of 34.4% (in HeLa) and 24.6% (in MCF-7) PI+ cells (necrotic cells) following 100  $\mu\text{M}$  of dimeric compound treatment for 48 h. Furthermore, this effect was selective, as healthy embryonic fibroblast cells remained unaffected by this treatment at the same concentrations and time-points (Fig. 7). The selectivity of dimeric compounds on cancer cells was further confirmed by the NucBlue Live staining, which was indicated by nuclear condensation and cell morphology. Since this assay indicates that dimeric compounds were effective at a 100  $\mu\text{M}$  dose in only cancerous cells, these compounds are thought to have a therapeutic potential, as they can be used reliably even at high doses without losing their selectivity (Fig. 8).

Intrinsic apoptosis or mitochondrial apoptosis signaling is a novel aim of several cancer therapy regimes including irradiation gamma chemotherapy, immunotherapy, and alternative medicine. For this reason, we analyzed gene expression belonging to both antiapoptotic and proapoptotic genes together with a tumor suppressor on the

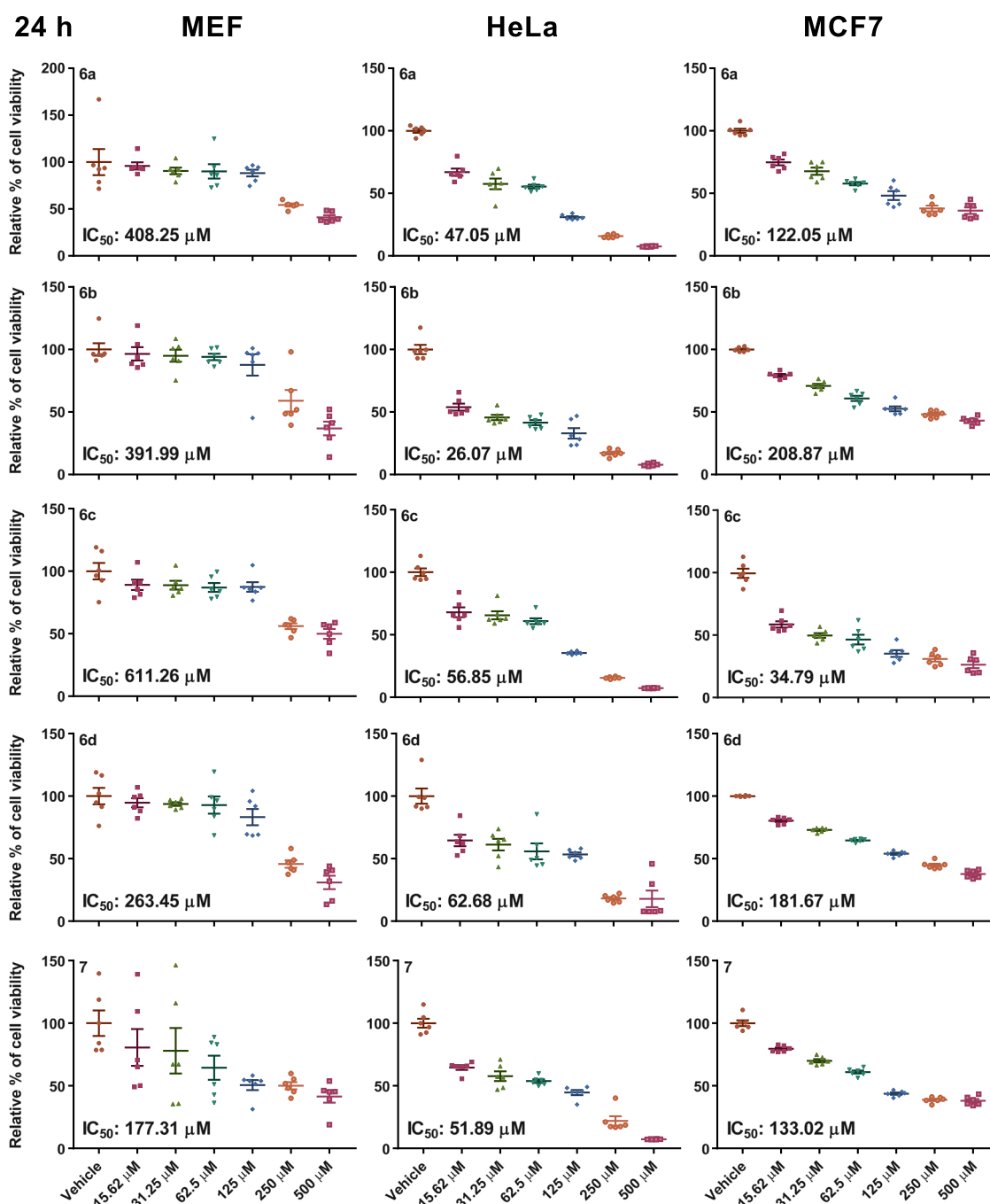


**Fig. 5** Cell viability in MEF; HeLa and MCF-7 cells treated with six different doses of ergosterol derivatives obtained by serial dilution starting from a 500  $\mu\text{M}$  dose for 24 h. All data are given as the mean

values of percentages for each group  $\pm$  SE.  $n = 6$ . MTT data at 24 h were used to calculate  $\text{IC}_{50}$  values using Probit analyses

mitochondrial apoptotic process in cervix and breast cancer cell lines to evaluate the effect of dimeric compound treatments on apoptotic cell death in HeLa and MCF-7.

The proapoptotic activity of tumor suppressor P53 has been recognized as apoptotic regulating the proapoptotic Puma, Noxa, and Bax proteins (Green and Kroemer 2004; Fulda and Debatin 2006). The expression of tumor suppressor P53 gene significantly increased only in **6b** (20.9-

fold) and **6c** (14.5-fold) treated HeLa cells and **6a** (41.83-fold), **6b** (2.35 fold), **6c** (4.1-fold), **6d** (23.3-fold) and treated MCF-7 cells, compared with the vehicle-treated control group (Fig. 5). Bcl-2 is an important apoptosis inhibitor protein and plays an important role in the protection of mitochondrial membrane potential. Its overexpression strongly prevents start of the apoptosis process in cells (Porter and Janicke 1999). The decrease in the ratio

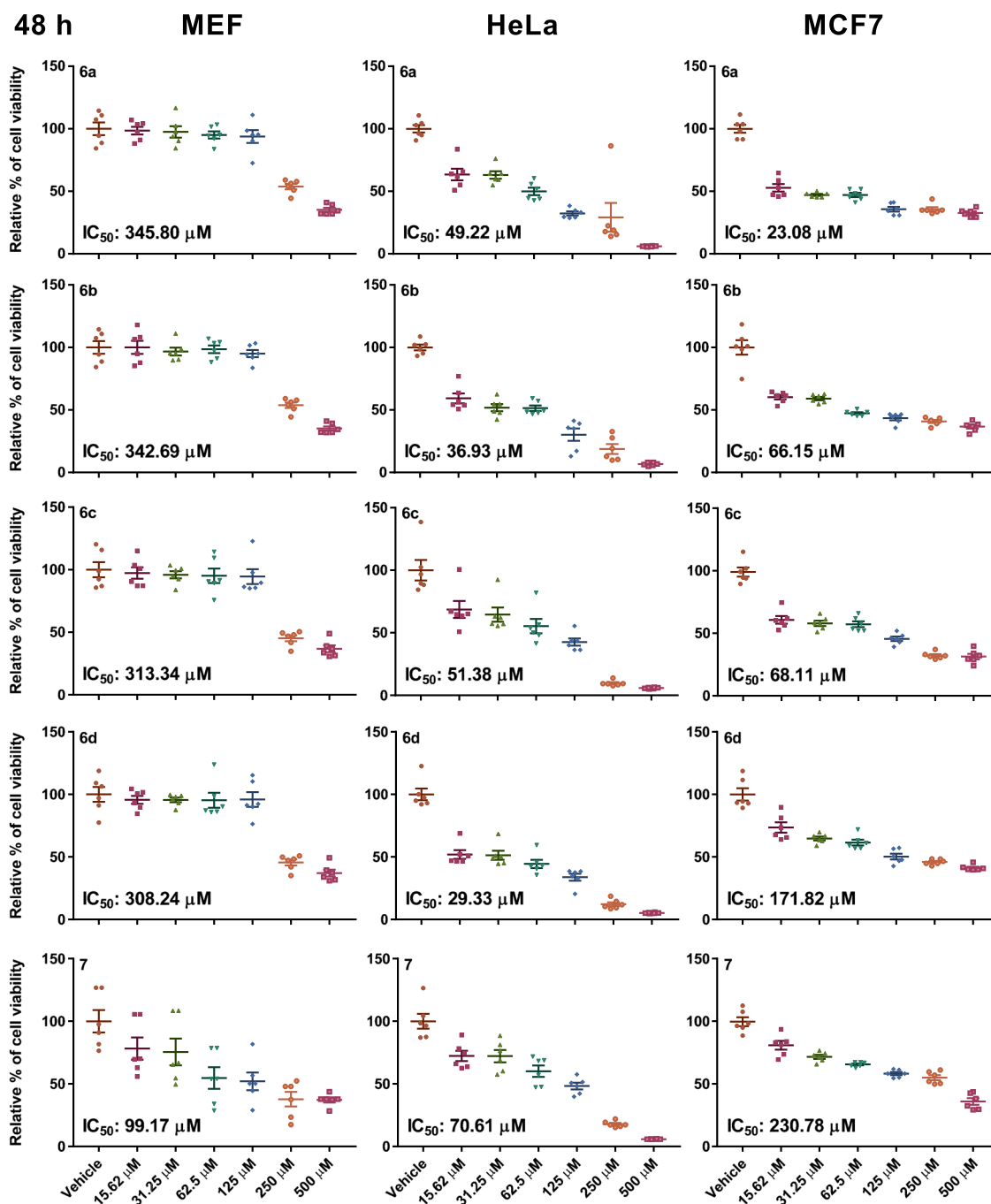


**Fig. 6** Cell viability in MEF; HeLa and MCF-7 cells treated with six different doses of ergosterol derivatives obtained by serial dilution starting from a 500 μM dose for 48 h. All data are given as the mean

values of percentages for each group ± SE. *n* = 6. MTT data at 48 h were used to calculate IC<sub>50</sub> values using Probit analyses

of Bcl-2 to BAX regulated by elevated BAX expression and Bcl-2 inhibition is an important initial factor of apoptosis (Li et al. 2013). BAX is a proapoptotic protein and its over-expression causes degradation of mitochondrial membrane potential and pore permeability (Fulda and Debatin 2006; Decaudin et al. 1998). A damaged mitochondrial membrane permits the release of Cytochrome-c to the cell cytosol, and this protein integrates with the APAF-1; then caspase 9

joins this complex and apoptosomes occur (Bratton et al. 2001; Cain et al. 2000). Apoptosome shows a high level of interest in caspase proteins. In this case, many caspase molecules are activated by this structure and an apoptosis cycle is completed.

Our results demonstrated that in HeLa cells while the cellular inhibitor of apoptosis gene Bcl-2 significantly expressed only the 6c-treated group, other dimeric

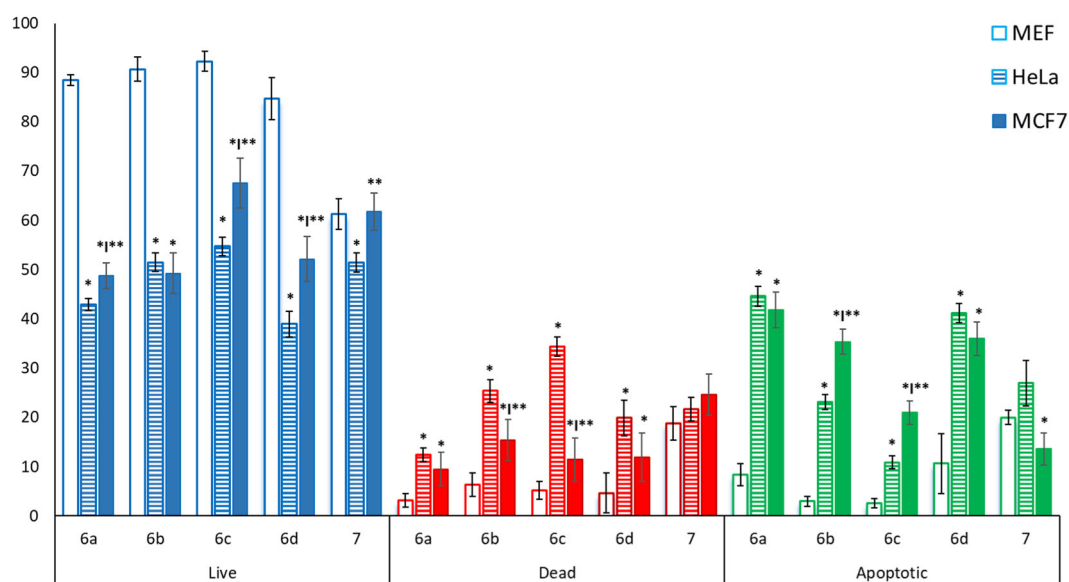


**Fig. 7** Percentage result of live, dead and apoptotic cells stained with Annexin V/propidium iodide as determined using a Tali image-based cytometer. All data are given as mean values of percentages for each group  $\pm$  SE.  $n = 6$ . An asterisk indicates significantly different values

compared with MEF cells analyzed by one-way ANOVA and Duncan test ( $p \leq 0.05$ ). Double asterisks indicate significantly different values compared with other cancerous cell lines ( $T$ -test:  $p \leq 0.05$ )

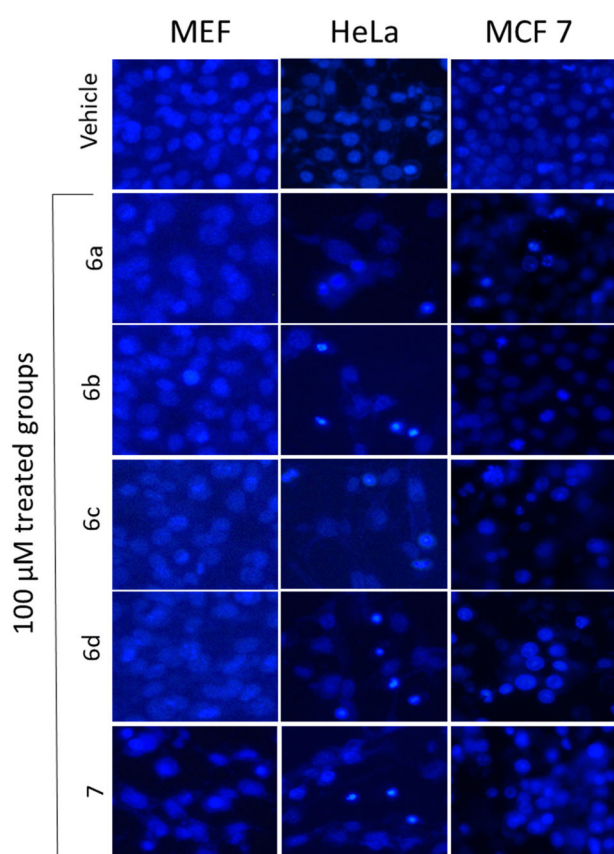


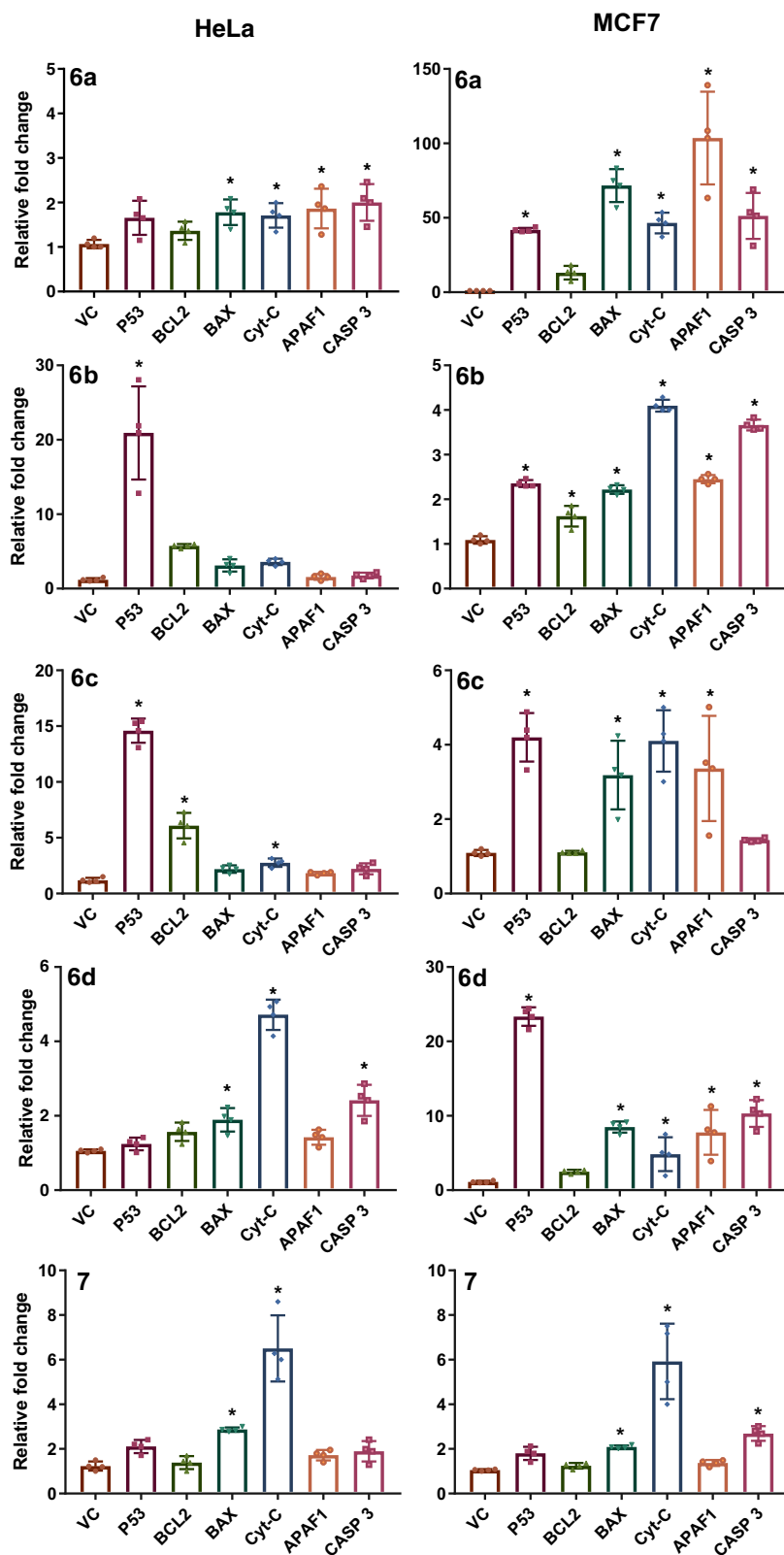
**Fig. 8** Apoptosis induction of 100  $\mu$ M dimeric compounds treatment in MEF, HeLa, and MCF-7 cells. Representative images of NucBlue live cell staining were shown blue color. Apoptotic cells exhibited morphological changes in the nuclei typical of apoptosis

compound-treated groups were placed at the same statistical level as the control. However, the Bcl-2/Bax ratio significantly decreased in **6a**- and **6d**-treated HeLa cells. In the MCF-7 cell line, dimeric compounds inhibited Bcl-2 and significantly triggered BAX expression in all experimental groups, except **7** treatment. A significant increase in the expression of Cyt-c was observed in **6a** and **6d** (1.7–4.8-fold) treated HeLa cells and almost all treated groups (4.11–46.5-fold) in MCF-7 cells. In the last step, the apoptosis biomarker Casp-3 overexpressed in both **6a** (2.0-fold) and **6d** (2.4-fold) treated HeLa cells and all the dimeric compound-treated group (2.7–51.2-fold) of breast cancer MCF-7 cells, except for the **6c** treatment (Fig. 9).

## Conclusions

In this study, four esters (**5a–d**) and five dimers (**6a–d**, **7**) out of nine novel compounds were synthesized. The structure of the obtained compounds was confirmed by FTIR,  $^1\text{H-NMR}$ ,  $^{13}\text{C-NMR}$ , and HRMS methods and their purity was determined by qNMR and HPLC. These dimeric compound's anticancer activities investigated against HeLa and MCF-7 cancer cell line and analyzed gene expression level on tumor suppressing cells for learning both anti-apoptotic and proapoptotic pathway. Biologic activity test results showed that the dimeric compounds synthesized in this study can selectively decrease the cell viability and proliferation in cervix cancer HeLa and breast cancer MCF-7 cells. However, in particular, the **7** derivative caused strong cytotoxicity in normal MEF cells. Therefore, we

**Fig. 9** Relative fold change qRT-PCR analysis of apoptosis pathway genes in IC<sub>50</sub> dose of -dimeric compounds treated MEF, HeLa, and MCF-7 cell lines for 48 h. All data were normalized with GAPDH expression and given as relative to the control (control = 1); *n* = 4. An asterisk indicates significantly different values were analyzed by one-way ANOVA and Duncan test (*p* ≤ 0.05)



consider that the use of this substance in cancer treatments is limited. In addition, other derivatives showed a very low cytotoxic effect on healthy cells. In this present study, we

report that the use of 100 μM concentrations of the dimeric compounds was sufficient in selectively inducing death and an apoptotic cell ratio in HeLa and MCF-7 breast cancer

cells. This indicates that **6a**, **6b**, and **6d** can act directly to induce apoptosis in both HeLa and MCF-7 cancer cells at relatively low IC<sub>50</sub> levels, unlike other derivatives for HeLa cells. These findings highlights that the **6a** derivative has potent antiproliferative and proapoptotic properties, in addition to **6d**. In conclusion, our results indicate that the obtained dimeric compounds are selective in inducing apoptotic cell death in breast cancer cells by targeting the p53-induced mitochondrial pathway. The same mechanism is observed only in **6a**, **6b**, and **6d** derivative-treated HeLa cells at 48 h. The effect of the number of carbon atoms on anticancer activity of the synthesized compounds was investigated but no significant effect was observed. In addition, although the presence of lithocholic acid moiety did not elevated programmed cell death on HeLa and MCF-7 cancer cell lines, it induced cytotoxic effect on normal cell MEF. Finally, we consider that the most effective dimeric compounds are **6a** and **6b**, which have the highest IC<sub>50</sub> value on healthy cells and the lowest IC<sub>50</sub> value in both cervix and breast cancer cells, especially in long-term treatment, and which specifically trigger the apoptosis pathway.

**Acknowledgements** This study was supported by Trakya University Scientific Research Projects Unit in projects number TUBAP 2015/72.

### Compliance with ethical standards

**Conflict of interest** The authors declare that they have no conflict of interest.

**Publisher's note** Springer Nature remains neutral with regard to jurisdictional claims in published maps and institutional affiliations.

### References

- Abdu-Allah HHM, Chang TT, Li W-S (2016) Synthesis of B- and C-ring-modified lithocholic acid analogues as potential sialyltransferase inhibitors. *Steroids* 112:54–61
- Ahmad TR, Haeusler RA (2019) Bile acids in glucose metabolism and insulin signalling-mechanisms and research needs. *Nat Rev Endocrinol* 15:701–712
- Anandkumar D, Rajakumar P (2017) Synthesis and anticancer activity of bile acid dendrimers with triazole as bridging unit through click chemistry. *Steroids* 125:37–46
- Asif M (2017) Pharmacological activities of Triazole analogues as antibacterial, antifungal, antiviral agents. *Pharm Sci Asia* 44:59–74
- Bratton SB, Walker G, Srinivasula SM, Sun XM, Butterworth M, Alnemri ES, Cohen GM (2001) Recruitment, activation and retention of caspases-9 and-3 by Apaf-1 apoptosome and associated XIAP complexes. *EMBO J* 20:998–1009
- Cain K, Bratton SB, Langlais C, Walker G, Brown DG, Sun XM, Cohen GM (2000) Apaf-1 oligomerizes into biologically active~700-kDa and inactive~1.4-MDa apoptosome complexes. *J Biol Chem* 275:6067–6070
- Campazzi E, Cattabriga M, Marvelli L, Marchi A, Rossia R, Pieragnoli MR, Fogagnolo M (1999) Organometallic radiopharmaceuticals: rhenium(I) carbonyl complexes of natural bile acids and derivatives. *Inorg Chim Acta* 286:46–54
- Chen J, Liu C-F, Yang C-W, Zeng C-C, Liu W, Hu L-M (2015) Design and synthesis of 5-chloro-2-hydroxy-3-triazolylbenzoic acids as HIV integrase inhibitors. *Med Chem Res* 24:2950–2959
- Dang Z, Jung K, Qian K, Lee K-H, Huang L, Chen C-H (2012) Synthesis of lithocholic acid derivatives as proteasome regulators. *ACS Med Chem Lett* 3:925–930
- Decaudin D, Marzo I, Brenner C, Kroemer G (1998) Mitochondria in chemotherapy-induced apoptosis: a prospective novel target of cancer therapy. *Int J Oncol* 12:141–193
- Duan T, Fan K, Fu Y, Zhong C, Chen X, Peng T, Qin J (2012) Triphenylamine-based organic dyes containing a 1,2,3-triazole bridge for dye-sensitized solar cells via a 'Click' reaction. *Dyes Pigm* 94:28–33
- El Kihel L, Clément M, Bazin MA, Descamps G, Khalid M, Rault S (2008) New lithocholic and chenodeoxycholic piperazinylcarboxamides with antiproliferative and pro-apoptotic effects on human cancer cell lines. *Bioorg Med Chem* 16:8737–8744
- Fulda S, Debatin KM (2006) Extrinsic versus intrinsic apoptosis pathways in anticancer chemotherapy. *Oncogene* 25:4798–4811
- Gafar AA, Draz HM, Goldberg AA, Bashandy MA, Bakry S, Khalifa MA, Sanderson JT (2016) Lithocholic acid induces endoplasmic reticulum stress, autophagy and mitochondrial dysfunction in human prostate cancer cells. *PeerJ* 4:e2445
- Glowacka IE, Balzarini J, Wróblewski AE (2013) The synthesis, antiviral, cytostatic and cytotoxic evaluation of a new series of acyclonucleotide analogues with a 1,2,3-triazole linker. *Eur J Med Chem* 70:703–722
- Goldberg AA, Beach A, Davies GF, Harkness TA, Leblanc A, Titorenko VI (2011) Lithocholic bile acid selectively kills neuroblastoma cells, while sparing normal neuronal cells. *Oncotarget* 2:761–782
- Goldberg AA, Titorenko VI, Beach A, Sanderson JT (2013) Bile acids induce apoptosis selectively in androgen-dependent and -independent prostate cancer cells. *PeerJ* 1:e122
- Green DR, Kroemer G (2004) The pathophysiology of mitochondrial cell death. *Science* 305:626–629
- Guclu H, Doganlar ZB, Gurlu VP, Ozal A, Dogan A, Turhan MA, Doganlar O (2018) Effects of cisplatin-5-fluorouracil combination therapy on oxidative stress, DNA damage, mitochondrial apoptosis, and death receptor signalling in retinal pigment epithelium cells. *Cutan Ocul Toxicol* 37:291–304
- He XL, Xing Y, Gu X-Z, Xiao J-X, Wang Y-Y, Yi Z, Qiu W-W (2017) The synthesis and antitumor activity of lithocholic acid and its derivatives. *Steroids* 125:54–60
- Himo F, Demko ZP, Noodleman L, Sharpless KB (2002) Mechanisms of tetrazole formation by addition of azide to nitriles. *J Am Chem Soc* 124:12210–12216
- Himo F, Lovell T, Hilgraf R, Rostovtsev VV, Noodleman L, Sharpless KB, Fokin VV (2005) Copper(I)-catalyzed synthesis of azoles. DFT study predicts unprecedented reactivity and intermediates. *J Am Chem Soc* 127:210–216
- Hryniewicka A, Łotowski Z, Seroka B, Witkowski S, Morzycki JW (2018) Synthesis of a cisplatin derivative from lithocholic acid. *Tetrahedron* 74:5392–5398
- Juráček M, Dzubák P, Sedlák D, Dvoráková H, Hajdúch M, Bartunek P, Drašar P (2013) Preparation, preliminary screening of new types of steroid conjugates and their activities on steroid receptors. *Steroids* 78:356–361
- Kádár Z, Molnár J, Schneider G, Zupkó I, Frank É (2012) A facile 'click' approach to novel 15 $\beta$ -triazolyl-5 $\alpha$ -androstane derivatives, and an evaluation of their antiproliferative activities in vitro. *Bioorg Med Chem* 20:1396–1402

- Kolb HC, Sharpless KB (2003) The growing impact of click chemistry on drug discovery. *Drug Discov Today* 8:1128–1136
- Li SZ, Zhang HH, Zhang JN, Zhang ZY, Zhang XF, Zhang XD, Du RL (2013) ALLN hinders HCT116 tumor growth through Bax-dependent apoptosis. *Biochem Biophys Res Commun* 437:325–330
- Lima-Neto RG, Cavalcante NNM, Srivastava RM, Mendonça Jr FJB, Wanderley AG, Neves RP, dos Anjos JV (2012) Synthesis of 1,2,3-triazole derivatives and in vitro antifungal evaluation on candida strains. *Molecules* 17:5882–5892
- Luchetti F, Canonico B, Curci R, Battistelli M, Mannello F, Papa S, Falcieri E (2006) Melatonin prevents apoptosis induced by UV-B treatment in U937 cell line. *J Pineal Res* 40:158–167
- Luu TH, Bard J-M, Carbonnelle D, Chaillou C, Huvelin J-M, Bobin-Dubigeon C, Nazih H (2018) Lithocholic bile acid inhibits lipogenesis and induces apoptosis in breast cancer cells. *Cell Oncol* 41:13–24
- Malkoch M, Thibault RJ, Drockenmuller E, Messerschmidt M, Voit B, Russell TP, Hawker CJ (2005) Orthogonal approaches to the simultaneous and cascade functionalization of macromolecules using click chemistry. *J Am Chem Soc* 127:14942–14949
- Menendez C, Gau S, Lherbet C, Rodriguez F, Inard C, Pascad MR, Baltas M (2011) Synthesis and biological activities of triazole derivatives as inhibitors of InhA and antituberculosis agents. *Eur J Med Chem* 46:5524–5531
- Morales-Sanfrutos J, Ortega-Munoz M, Lopez-Jaramillo J, Hernandez-Mateo F, Santoyo-Gonzalez F (2008) Synthesis of calixarene-based cavitations and nanotubes by click chemistry. *J Org Chem* 73:7768–7771
- Nagesh HN, Suresh N, Prakash GVSB, Gupta S, Rao JV, Sekhar KVG (2015) Synthesis and biological evaluation of novel phenanthridinyl piperazine triazoles via click chemistry as antiproliferative agents. *Med Chem Res* 24:523–532
- Narayanaswamy N, Maity D, Govindaraju T (2011) Reversible fluorescence sensing of Zn<sup>2+</sup> based on pyridine-constrained bis(triazole-linked hydroxyquinoline) sensor. *Supramol Chem* 23:703–709
- Nascimento PGG, Lemos TLG, Almeida MCS, Souza JMO, Bizerra AMC, Santiago GMP, Costa JGM, Coutinho HDM (2015) Lithocholic acid and derivatives: antibacterial activity. *Steroids* 104:8–15
- Nejma AB, Znati M, Daich A, Othman M, Lawson AM, Jannet HB (2018) Design and semisynthesis of new herbicide as 1,2,3-triazole derivatives of the natural maslinic acid. *Steroids* 138:102–107
- Porter AG, Janicke RU (1999) Emerging roles of caspase-3 in apoptosis. *Cell Death Differ* 6:99–104
- Qiao D, Stratagouleas ED, Martinez JD (2001) Activation and role of mitogen-activated protein kinases in deoxycholic acid-induced apoptosis. *Carcinogenesis* 22:35–41
- Rahman M, Mohammad Y, Fazili KM, Bhat KA, Ara T (2017) Synthesis and biological evaluation of novel 3-O-tethered triazoles of diosgenin as potent antiproliferative agents. *Steroids* 118:1–8
- Ramírez-López P, de la Torre MC, Montenegro HE, Asenjo M, Sierra MA (2008) A straightforward synthesis of tetrameric estrone-based macrocycles. *Org Lett* 10:3555–3558
- Reddy VG, Bonam SR, Reddy TS, Akunuri R, Naidu VGM, Nayak VL, Bhargava SK, Kumar HMS, Srihari P, Kamal A (2018) 4β-amidotriazole linked podophyllotoxin congeners: DNA topoisomerase-IIα inhibition and potential anticancer agents for prostate cancer. *Eur J Med Chem* 144:595–611
- Rostovtsev VV, Green LG, Fokin VV, Sharpless KB (2002) A stepwise Huisgen cycloaddition process: copper(i)-catalyzed regioselective “ligation” of azides and terminal alkynes. *Angew Chem Int Ed* 41:2596–2599
- Salucci S, Burattini S, Battistelli M, Baldassarri V, Curzi D, Valmori A, Falcieri E (2014) Melatonin prevents chemical-induced haemopoietic cell death. *Int J Mol Sci* 15:6625–6640
- Tan W, Li Q, Gao Z, Qiu S, Dong F, Guo Z (2017) Design, synthesis of novel starch derivative bearing 1,2,3-triazolium and pyridinium and evaluation of its antifungal activity. *Carbohydr Polym* 157:236–243
- Vasilyeva SV, Shtil AA, Petrova AS, Balakhnin SM, Achigecheva PY, Stetsenko DA, Silnikov VN (2017) Conjugates of phosphorylated zalcitabine and lamivudine with SiO<sub>2</sub> nanoparticles: synthesis by CuAAC click chemistry and preliminary assessment of anti-HIV and antiproliferative activity. *Bioorg Med Chem* 25:1696–1702
- Vatmurge NS, Hazra BG, Pore VS, Shirazi F, Chavan PS, Deshpande MV (2008) Synthesis and antimicrobial activity of β-lactam-bile acid conjugates linked via triazole. *Bioorg Med Chem Lett* 18:2043–2047
- WCRF (2018), World Cancer Research Fund. American Institute for Cancer Research. Worldwide Cancer Data. <https://www.wcrf.org/dietandcancer/cancer-trends/worldwide-cancer-data> Accessed 24 January 2019
- Yadav P, Lal K, Kumar L, Kumar A, Kumar A, Paul AK, Kumar R (2018) Synthesis, crystal structure and antimicrobial potential of some fluorinated chalcone-1,2,3-triazole conjugates. *Eur J Med Chem* 155:263–274